MAP 2025 - Granular Entanglement

September 27, 2025

Abstract

Granular entanglement describes the jamming behavior that emerges from the overlap between convex hulls of non-convex grains. In this work, we identify grain-scale metrics responsible for granular entanglement in aggregates. Given an arbitrary, possibly non-convex grain shape, we propose numerical algorithms to compute grain-scale entanglement metrics such as accessibility and angular coverage in two and three dimensions. Using the PeriDEM framework, we perform bulk simulations of homogeneous granular aggregates of various parametrized families of non-convex grains, and quantify the relationship between the grain-scale metrics and the bulk entanglement indicators such as settling height. Our work allows for precise grain shape engineering to achieve a desired homogenized bulk property associated with structural resilience of granular aggregates.

Contents

1 Introduction

Granular media are materials composed of discrete solid particles, with solid-like or fluid-like behavior depending on their arrangement.

Granular entanglement has been of interest recently. In traditional Discrete Element Method (DEM) simulations of granular media fails to capture the complex contact modes observed in bulk simulations of non-spherical, especially of non-convex particle shapes. Recent developments of simulation techniques such as LS-DEM, Grains3D, and other DEM-based coupling approaches have enabled us to take into account the jamming behavior due to the shapes of the particles. In [3], the authors investigated the stability of freestanding columns made of U-shaped particles under vibration, demonstrating that intermediate barb length leads to maximum entanglement via interpenetration. In [1], the authors developed a hybrid PeriDEM simulation framework to study grain shape effects and damage under settling and compression. Although these studies mainly focus on the role of particle shape

in bulk behavior, few of them provide a quantitative metric of entanglement that is independent of the physical interaction parameters. Our work aims to fill this gap by introducing a geometric measure of inaccessibility, applicable across both 2D and 3D non-convex shapes, without relying on force-based modeling.

This work investigates how features of particle geometry such as accessible volume and angular coverage contribute to the degree of entanglement in a particle bulk. We propose accessibility as a metric for describing jamming behaviors associated with specific particle geometry in both two and three dimensions. Using bulk simulations such as settling under gravity, we establish a relationship between individual particle shape and bulk settling height. We found out that varying degrees of entanglement control structural stability, offering shape-driven cohesion for reconfigurable engineering structures without adhesives.

2 Entanglement of granular media

Granular jamming is an arrangement of grains where any rigid motion (rotation and translation) of any particle would lead to overlap. Notably, granular jamming is independent of friction and is a direct result of individual particle shape and particle arrangement. Granular jamming and jamming transition of circular particles have been studied In [3],[2].

We define granular entanglement as the overlap of the convex hulls of particles, ensuring there is no overlap between the particles. Naturally, it is characteristic of nonconvex particle shapes exclusively. To demonstrate this further, we list down a few definitions.

Definition 1. *Define a particle as a compact subset D of $\mathbb{R}^n$, where $n = 2$ or 3.*

Definition 2. *The convex hull $\overline{D}$ of particle D is defined as*

$$\overline{D} = \{\lambda \mathbf{x} + (1-\lambda)\mathbf{y} : \mathbf{x}, \mathbf{y} \in D,\ \lambda \in [0,1]\}.$$

Definition 3. *Two particles $D_1, D_2 \subset \mathbb{R}^n$ are said to be entangled if*

$$D_1 \cap D_2 = \phi \text{ and } \overline{D_1} \cap \overline{D_2} \neq \phi,$$

where ϕ is the empty set.

In a large granular aggregate of irregular shapes, the particles are assumed to be oriented randomly. For regular shapes such as spheres and regular polygons, bulk settling experiments under uniform body force such as gravity exhibit crystallization, where particles arrange in an ordered fashion on a lattice grid. This is not the case for irregular shapes with lack of spherical or dihedral symmetry. In this case, the particles are assumed to be oriented randomly in a bulk.

2.1 Design of parametric family of shapes

To investigate the configurations in which two non-convex objects could lie on a fixed surface without overlapping, we consider three simple non-convex shapes: *pacman*, *C-shape* and *plus-shape* (see Figure 1).

A classical *pacman* can be constructed by the set the difference of a disk and a triangle. A C-shape is built by forming an circle with outer radius R and another with inner radius r, taking the union of them then cutting of the variable *mouth angle* ϕ. For the *Plus-shape*, it is a cross shape at the center, built by removing four identical small square from A big square, added by four identical arms on each side. The parameter is the transverse arm. Fix the 2D plane as a 5 cm $\times$ 5 cm grid.

(add more detailed description of design for c, pacman, and cross shapes. done)

2.2 Metric for entanglement

First we consider the 2D case for simplicity. We assume that two identical particles are free to move around in a 2D plane. We assume the particles go through rigid motions only. Particle deformation due to elasticity, plasticity, or fracture are ignored here.

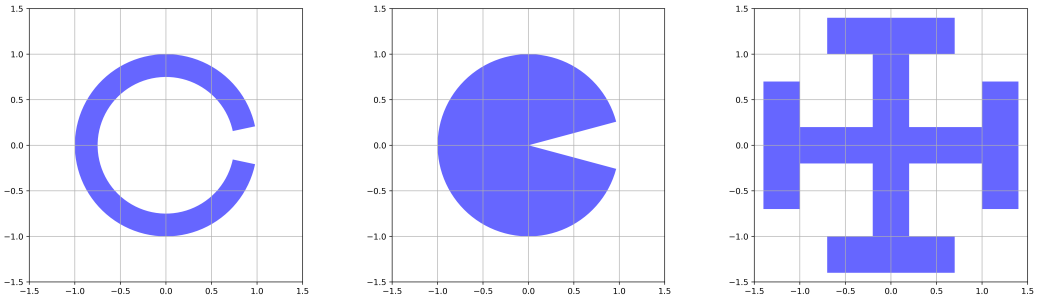

(a) C-shaped particle (b) Pacman-shaped particle (c) Cross-shaped particle

Figure 1: Non-convex shapes considered

Definition 4. *The current particle $D_{\theta,\mathbf{z}}$ due to a counterclockwise rotation by an angle $\theta \in [0, 2\pi]$ followed by a translation by a vector $\mathbf{z} \in \mathbb{R}^2$ of particle $D \in \mathbb{R}^2$ is given by*

$$D_{\theta,\mathbf{z}} = \{\mathbf{z} + R_\theta \mathbf{x} : \mathbf{x} \in D\},$$

where $R_\theta \in \mathbb{R}^{2\times 2}$ is the rotation matrix given by

$$R_\theta = \begin{bmatrix} \cos\theta & -\sin\theta \\ \sin\theta & \cos\theta \end{bmatrix}.$$

Definition 5. *The accessible area associated with particle $D \in \mathbb{R}^2$ is defined as the union of all regions that can be occupied by another identical particle without overlapping with the the original particle. More precisely,*

$$Acc(D) = \bigcup_{(\theta,\mathbf{z})\in[0,2\pi]\times\mathbb{R}^2} \{D_{\theta,\mathbf{z}} : D_{\theta,\mathbf{z}} \cap D = \phi\}.$$

For a parametrized family of particle shape, a change in parameter (e.g. mouth angle for pacman-shaped particles) leads to the area of the particle. To account for this, we consider the ratio of accessible area with respect to the total area of the convex hull associated with the shape.

Definition 6 (Accessibility)**.** *We define the accessibility A_a of a particle D_a with parameter $a \in \mathbb{R}$ as the ratio of its accessible area within its convex hull, i.e.*

$$A_a = \frac{|Acc(D_a) \cap \overline{D_a}|}{|\overline{D_a}|} \tag{1}$$

We also define a new variable called inaccessibility (I_a) representing the ratio of inaccessible area for the other shape to reach compared to the total area of the convex hull. Here the convex hull is the area covered by the outer radius R. The inaccessible area inside the convex hull we called a_iThus we have

$$I_a = \frac{a_i}{\pi R^2} \tag{2}$$

2.3 Numerical method

For a general non-convex particle, an analytical method for computing the accessibility is intractable. We used a computational program to construct all the possible rotations and translations for which objects do not overlap with each other. We combine the area together and name it as *accessible area*. We set the first shape at the origin of the grid, then translate the other shape across all regions throughout the grid. We design an algorithm to compute this whole area throughout the grid. We plot this area with a contrasting area, defining the colored area as accessible area, while the white (empty) parts are inaccessible, meaning that another pacman could not be placed within that region.

Algorithm 1 Compute Accessibility I vs. Mouth Angle ϕ for Pac-Man Shape

Initialize: $\phi \leftarrow 0$ to 95 in steps of 2
Initialize: $I_{\text{values}} \leftarrow [\,]$
Define convex hull $\mathcal{B}$ as unit circle
Define inner hole as fixed circle of radius 0.75
    This algorithm specify how the same shape with different mouth angle would lead to different accessibility
for each ϕ in $\{0, 2, 4, \ldots, 90\}$ **do**
    Generate Pac-Man shape $\mathcal{S}_1$ with mouth angle ϕ
    Subtract inner circle from $\mathcal{S}_1$ to form $\mathcal{S}_{\text{pac}}$
    $V \leftarrow \emptyset$ ▷ Valid placements
    for each x in $[-2.5, 2.5]$ step 0.2 **do**
        for each y in $[-2.5, 2.5]$ step 0.2 **do**
            for each angle θ in $[0°, 360°]$ step 5° **do**
                Rotate $\mathcal{S}_{\text{pac}}$ by θ to get $\mathcal{S}'$
                Translate $\mathcal{S}'$ by (x, y)
                if $\mathcal{S}'$ does not intersect $\mathcal{S}_{\text{pac}}$ **then**
                    Add $\mathcal{S}'$ to V
                end if
            end for
        end for
    end for
    Compute union of all shapes in V: $\mathcal{U} \leftarrow \bigcup V$
    Compute accessible area inside boundary: $\mathcal{A} \leftarrow \mathcal{B} \cap \mathcal{U}$
    $I \leftarrow \text{area}(\mathcal{A})/TotalArea$
    Append I to I_{values}
end for
Plot I_{values} against ϕ

We may draw the graph through Matplotlib on Inaccessibility vs Pac-Man Mouth angle, balancing the computational time and precision, we perform a step size of 2 degrees from 0-95 degrees.

2.4 MPI compatible version of accessibility code

We used parallel computing using the Message Passing Interface (MPI) framework to accelerate the simulation process, implemented in Python with the mpi4py library. This allowed us to distribute the computational workload across multiple CPU cores. Each core, referred to as a "rank", was assigned a subset of the mouth angle values (ϕ) to process.

(Add accessible plots for pacman, done)

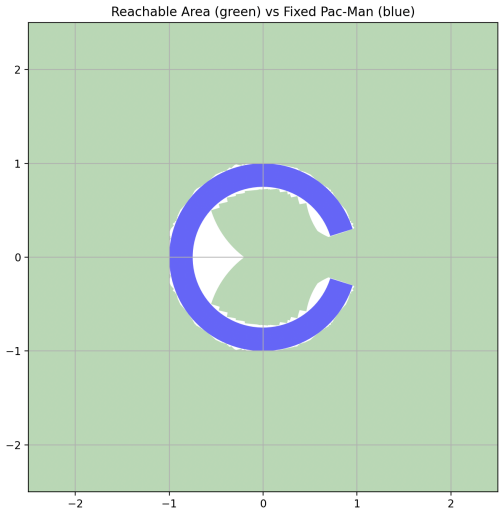

Figure 4: The accessible area of a C shape on a grid

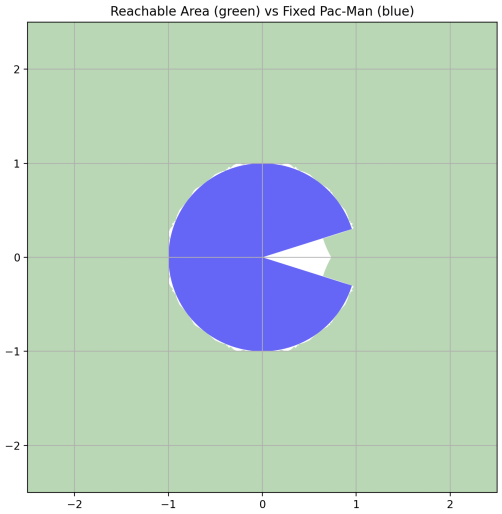

Figure 5: The accessible area of a pacman shape on a grid

3 Discontinuity in accessibility with respect to shape parameter

4 Particle entanglement in 3D

3D particles obtained from extruding 2D shapes exhibit less granular entanglement due to the additional degree of freedom. In 3D, the rigid motion of the particle $D \in \mathbb{R}^3$ can be characterized by a vector $\Theta = (\theta_x, \theta_y, \theta_z) \in \mathbb{R}^3$ of rotation about the x, y, and z axes by an angle θ_x, θ_y, and θ_z, respectively, and a translation vector $\mathbf{z} \in \mathbb{R}^3$. Therefore, the current particle $D_{\Theta,\mathbf{z}} \in \mathbb{R}^3$ after undergoing a rigid motion can be described as

$$D_{\Theta,\mathbf{z}} = \{\mathbf{z} + R_\Theta \mathbf{x} : \mathbf{x} \in D\},$$

where the rotation matrix R_Θ with defined as

$$R_\Theta = R^x_{\theta_x} R^y_{\theta_y} R^z_{\theta_z} \in \mathbb{R}^{3\times 3}$$

where

$$R^x_{\theta_x} = \begin{bmatrix} 1 & 0 & 0 \\ 0 & \cos\theta_x & -\sin\theta_x \\ 0 & \sin\theta_x & \cos\theta_x \end{bmatrix}, \; R^y_{\theta_y} = \begin{bmatrix} \cos\theta_y & 0 & -\sin\theta_y \\ 0 & 1 & 0 \\ \sin\theta_y & 0 & \cos\theta_y \end{bmatrix} . R^z_{\theta_z} = \begin{bmatrix} \cos\theta_z & -\sin\theta_z & 0 \\ \sin\theta_z & \cos\theta_z & 0 \\ 0 & 0 & 1 \end{bmatrix} .$$

The accessible area associated with particle $D \in \mathbb{R}^3$ is defined as the set

$$Acc(D) = \bigcup_{(\Theta,\mathbf{z})\in[0,2\pi]^3\times\mathbb{R}^3} \{D_{\Theta,\mathbf{z}} : D_{\Theta,\mathbf{z}} \cap D = \phi\} .$$

4.1 3D shapes

We created a set of three-dimensional shapes to examine how the geometry of particles may impact the entanglement of granular media. In the next part, we will perform a real simulation and 3D collision using these forms, which reflect varying degrees of geometric complexity and interlocking potential. Listed below are the example objects:

• The 3D Pacman is generated based on the 2D shape we defined in Part 3. We generated a whole sphere and cut off a piece of "cheese" shape from it to imitate the "mouth".

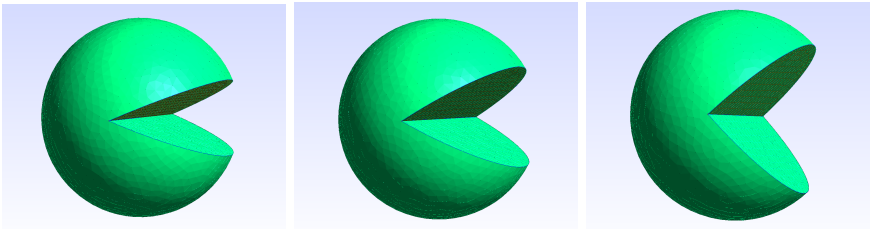

Figure 6: Pacmen with mouth angles: 45°, 60°, 90°

• "Dumbbells" are made up of three cuboids – the two "hands" and a neck. The two hands are placed on the sides perpendicular to each other, connected by the center 'neck'. The length of neck and hands is the primary adjustable parameter that controls how easily the objects can hook or slip past one another when multiple of them are placed together. Geometric interlocking in packaging may result from this.

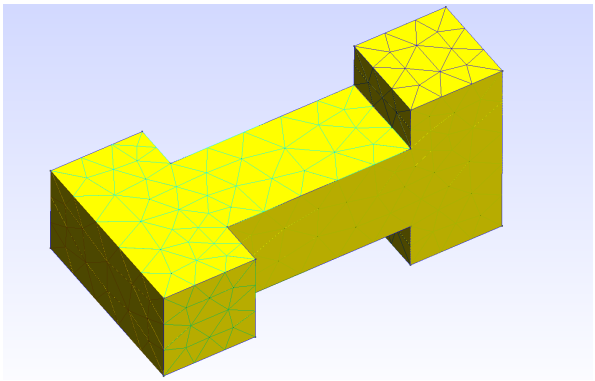

Figure 7: 3-D Dumbbell Shape

• Branch-shaped objects consist of a central body with four or more branches extending outward, follow with "shells" on the top of each branch. and their key adjusted parameters are length, thickness and angular separation. This design introduces multiple potential contact points and significantly

increases the likelihood of entanglement. The two shapes we invented here were inspired by the structure of a virus, which extended arms enhance frictional and topological locking. As shown in Figures [5] and [6], the block shape branches are cuboids, the top of each branch is a flat square surface cut from the original cube, which is the cube with a radius equal to the length of the branch. For the sphere, the branches are cylinders, with top shells, or hats, cut from the original sphere also with radius the same as the branched.

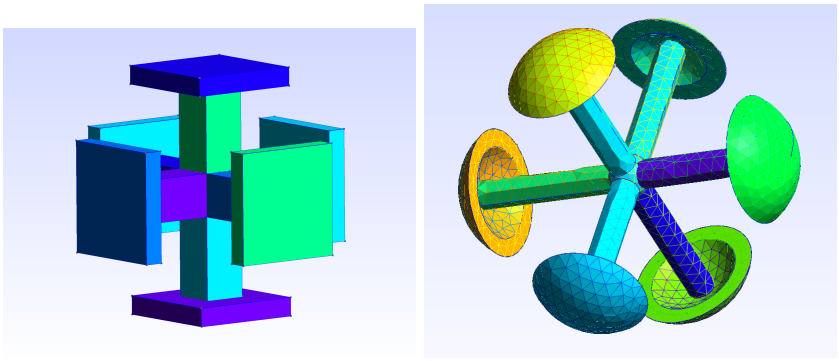

Figure 8: 3D Cube and Sphere

4.2 3D Metric

After testing the idea of entanglement, defining convex hulls and "inaccessibility", we expand the same framework into 3D models, particularly on the 3D Pacman as introduced earlier. Using Gmsh as both the modeling and visualization tool, we first generated a "base Pacman" at the base with *mouthangle* defined as ϕ.

To evaluate how densely the identical objects can be packed around the base pacman, we systematically duplicate many of the identical pacmen around it (marked as B), doing translational and rotational scanning over a sufficiently large cubic area. The translation parameters dx, dy, and dz, spanned in the range $[-1, 1]$ with a step size 6. The rotation parameters are ϕ_x, ϕ_y, and ϕ_z referring to the three axis, rotated every 6 degrees. For each copy, a boolean intersection check is applied to determine if it intersects with the base pacman. if there was no intersection, the copy was considered valid and been kept.

After generating enough number of Bs, most of the area around the base pacman will be covered, but there will likely be a small irregular space around the "mouth" which no addition pacman can achieve. Then we call that the "inaccessible area". The inaccessible area can be calculated using the difference between the mouth volume and the accessible area.

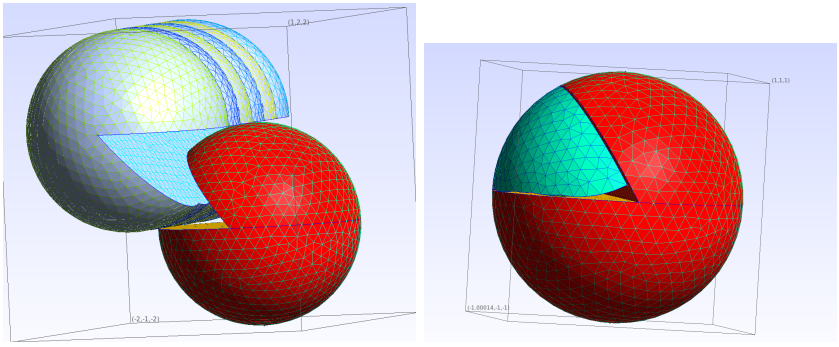

Figure 9: 3D Cube and Sphere

5 Bulk Simulation of parametrized families of grain shapes

To perform bulk simulations of the parametrized families of shapes described in Section 2.1, we utilize the PeriDEM framework introduced in [4, 1]. The method combines a short-range contact forces to account for inter-particle forces, similar to the Discrete Element Method (DEM), and peridynamics [5] to account for the intra-particle deformation and even breakage of each grain. The nonlocal approach allows for capturing accurate contact between highly complex non-convex shapes in a granular aggregates. In this work, extreme deformation such as breakage is not of interest. Additionally, we ignore the effect of deformation by considering sufficiently stiff material properties (see table) .

The bulk simulations are designed to investigate how the geometry and topology of the particles influence the macroscopic behavior of granular materials under gravitational settling and external compression. We perform bulk simulations using a custom hybrid numerical framework *perigrain*. Our simulations are implemented in C++ and run in parallel using MPI across 40 CPU cores on the Grinnell College high-performance computing cluster. Each simulation begins by initializing a set of 400 identical non-convex particles within a rectangular container. The particles are defined through polygonal approximations (2D) and are discretized into finite number (around 11000) of nodes (how many? done) .

We aim to discover the relationship between accessibility and the change of height of a bulk setup. We let the particles fall freely under gravity and letting them settle until the reach an equilibrium (until the kinetic energy of the bulk vanishes). (Edit following sentences. done) For the 2D cross shape with hook length set to 0.5, after a time step of $dt = 8 \times 10^{-8}$ and 63,000 simulation steps, the system eventually relaxes as the contact number ceases to change. The damping coefficient is set to 0.95. The mesh size is given by $1 \times 10^{-3}/10$, with 10 used as the mesh size factor.

Shape	**Cross(left)**	**Cross(right)**
hook length	0.5	0.1
arm length	0.72	0.70
meshsize	1e-4	6.66e-5
damping ratio	0.95	0.95
dt	8e-8	8e-8

Table 1: Comparison of accessibility and entanglement for different non-convex shapes.

A similar simulation is produced for longer head particles (the outer surface of each edge is similar), but the meshsize should be smaller 1e-3/15.

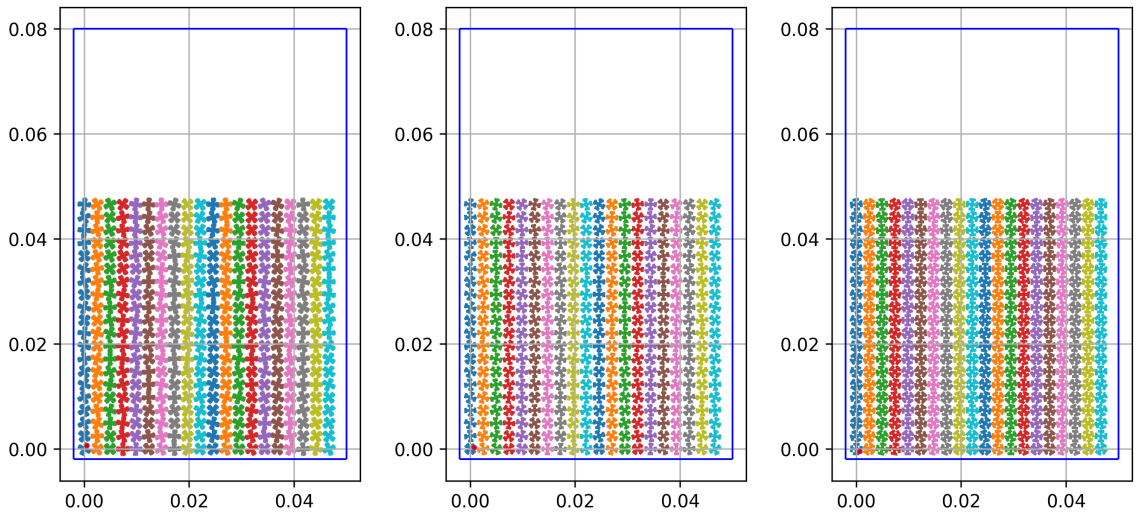

Figure 10: shorter head (left) vs longer head (bottom) middle head(right) 2d "Crosses"

And afterwards, the result shows below that the left is 3d cross with a shorter head while the right

is 3d cross with relatively longer head.

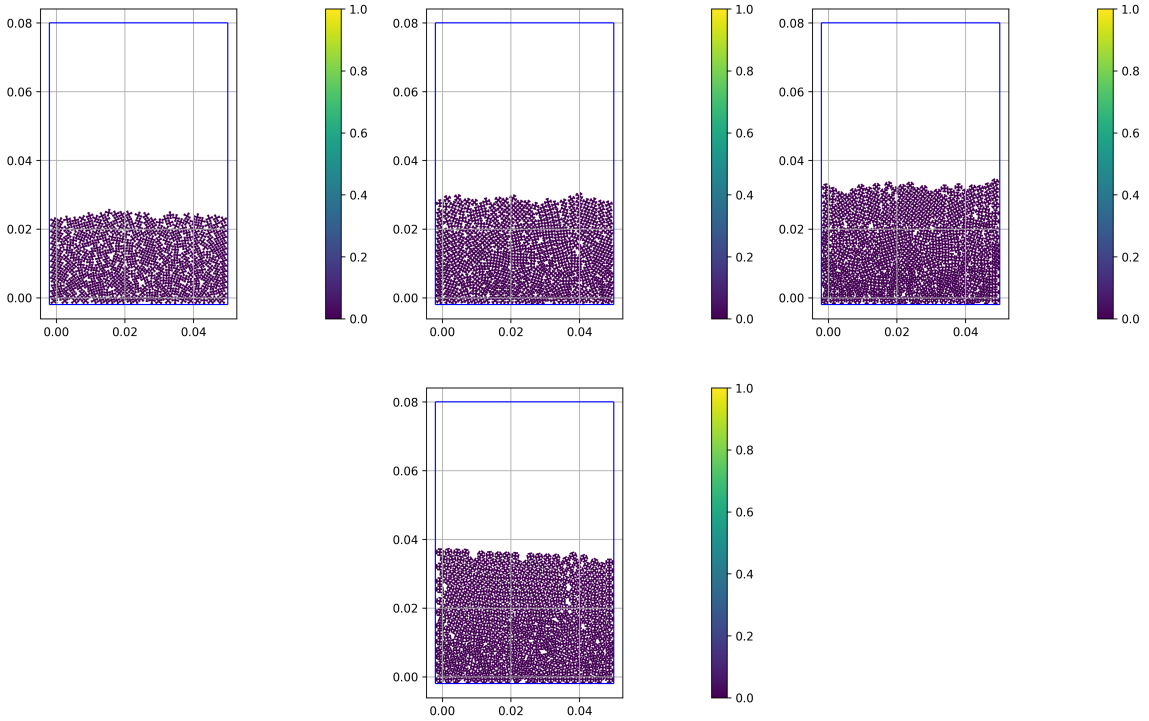

Figure 11: shorter head (left) vs longer head (bottom), middle head(right) 2d "Crosses"

A similar simulation is produced for longer head particles (the outer surface of each edge is similar), but the meshsize should be smaller 1e-3/15.

In order to analyze the result, we try to plot the relationship between inaccessibility with the height difference between before and after the relaxation process of the bulk. Running each of the simulations till settling with 4 nodes, 20 cores per node, it takes approximately 2 hours to complete the run section of the code.

Shape	**Hook length 1**	**Hook length 0.75**	**Hook length 0.5**
Inaccessibility	0.0473	0.0166	0.0078
Height change	0.014	0.019	0.023

Table 2: Comparison of accessibility and entanglement for different non-convex shapes.

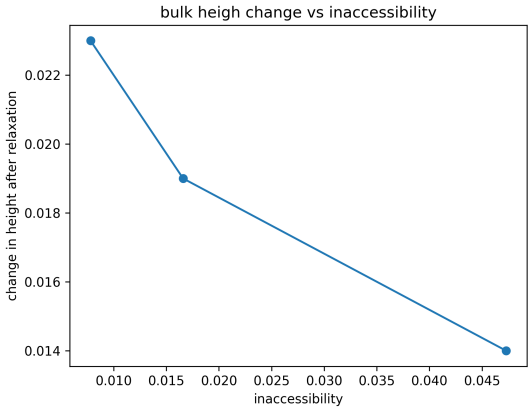

Figure 12: The Relationship Between Inaccessibility and Height change

Combining the visual result of the bulk's configuration after the relaxtion and analysis of the numerical value of height change, we confirm our hypothesis that

6 Summary

6.1 Result

We summarize our results as follows.

1. By evaluating the nonconvex geometries including C, pacman, and cross shapes both in 2D and 3D, we quantify the relationship between opening angles, accessibility, and bulk granular entanglement.
2. For 2D shapes, the accessible area increases with the mouth angle ϕ. Same for the cross shape, the shorter the hook length, the larger the angle, the larger the accessibility.
3. For 3D, we extended the same method by scanning translated and rotated copies around a base pacman particle. Inaccessible volumes were concentrated near the mouth region.
4. For bulk simulations, the result shows that the shape with shorter head length lead to lower height, representing stronger degree of entanglement.

6.2 Conclusion and future directions

Our current result confirms that granular accessibility is a metric closely related to changes in geometry and reflects the degree of openness of the structures. Considering settling height as a measure of entanglement, our simulations suggest that accessibility may be able to predict interlocking behavior. Further work will focus on 3D equivalent of similar problems.

References

[1] D. Bhattacharya and R. Lipton. Simulating grain shape effects and damage in grannular media using peridem. *SIAM Journal on Computing*, 45(1):B1–B26, 2023.

[2] D. Bhattacharya and R. Lipton. Macroscopic effects of intraparticle fracture, grain topology and shape on vehicle dynamics and mobility over gravel road beds. *Granular Matter*, 27(1):2, 2025.

[3] N. Gravish, S. V. Franklin, D. L. Hu, and D. I. Goldman. Entangled Granular Media. *Physical Review Letters*, 108(20):208001, May 2012.

[4] P. K. Jha, P. S. Desai, D. Bhattacharya, and R. Lipton. Peridynamics-based discrete element method (PeriDEM) model of granular systems involving breakage of arbitrarily shaped particles. *Journal of the Mechanics and Physics of Solids*, 151:104376, June 2021.

[5] S. A. Silling. Reformulation of elasticity theory for discontinuities and long-range forces. *Journal of the Mechanics and Physics of Solids*, 48(1):175–209, Jan. 2000.

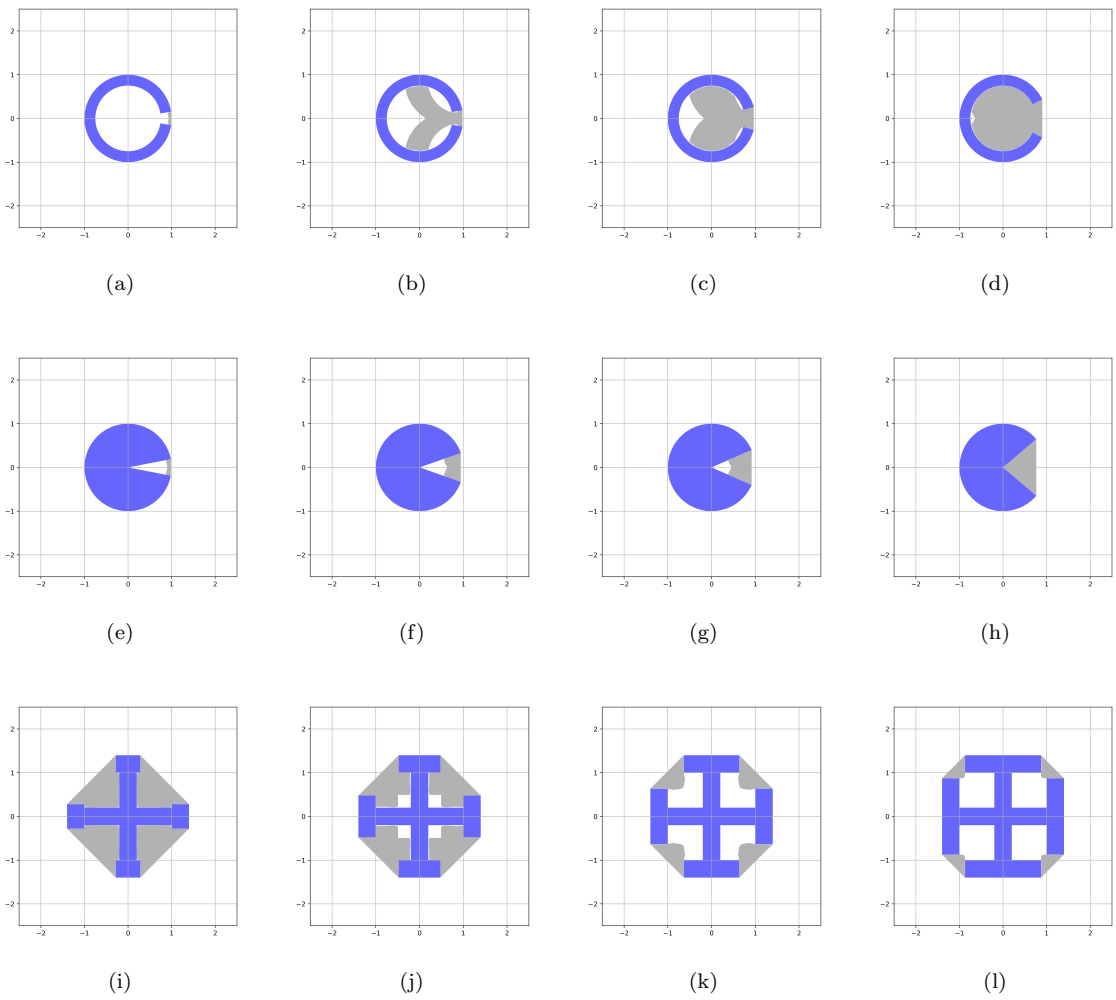

Figure 2: Accessible area within the convex hulls of particles are are shown in gray. (a) - (d): C-shaped with mouth angle as the parameter. (e)-(h): pacman-shaped particles with mouth angle and the parameter. (i) - (l): cross-shaped particles with hook length as the parameter. For pacman and C-shaped particles, accessible volume is monotonic in mouth angle, i.e., a lower mouth angle leads to a reduced accessible area within the convex hull of the nonconvex shape. The mouth angle of the c-shapes are 20°, 30°, 40° and 60°. The mouth angle of the pacmans are 20°, 40°, 60° and 90°. For the cross shapes, set the half bar length(from the center to edge, not included the outer edges) as 1. The hook lengths are 1/3, 3/4, 1, 1.5 (Include the mouth angle and hook length for each shape, done)

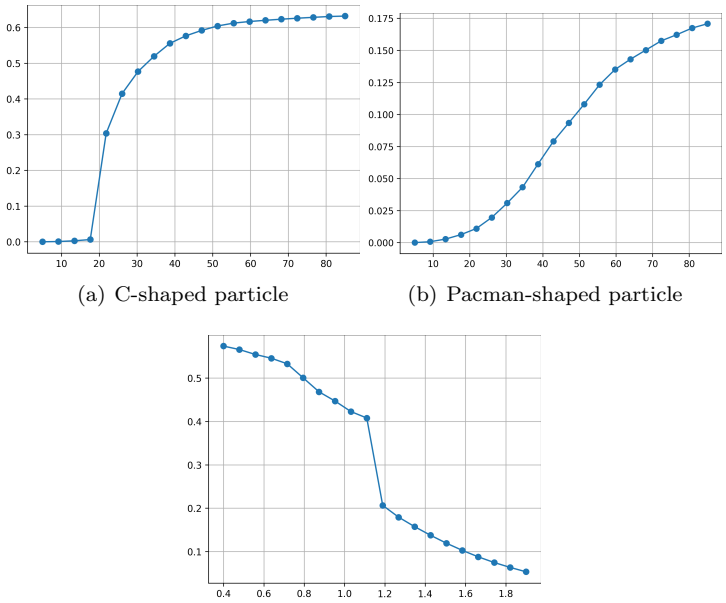

(a) C-shaped particle (b) Pacman-shaped particle

(c) Cross-shaped particle

Figure 3: Accessibility A_a vs the shape parameter for each non-convex shape. The x-axis for C and pacman-shaped particles are mouth angle $a \in [0, \pi]$, and hook length $a \in [0.4, 2.0]$ for cross-shaped particles.